Efficient Solution and Performance Analysis of 3-D Position Estimation by Trilateration

DIMITRIS E. MANOLAKIS, Member, IEEE
Sithon Research
and Hellenic Air Force Academy

A new exact, explicit, and computationally efficient solution for three-dimensional (3-D) position estimation based on range measurements from three stations is proposed. The simple polynomial-type form of the new algorithm facilitates the performance analysis. Formulae are provided for both the variance and the bias of the position estimates. The systematic error is a joint effect of both the measurement noise and the system nonlinearity and its magnitude cannot be ignored if highly accurate localization is required. Performance evaluation results are presented for various conditions.

Manuscript received November 18, 1993; revised February 28, 1995.

IEEE Log No. T-AES/32/4/07993.

Author's current address: Dept. of Automation, TEI of Thessaloniki, P.O. Box 14561, Thessaloniki 54101 Greece.

I. INTRODUCTION

Trilateration is a method to determine the position of an object based on simultaneous range measurements from three stations located at known sites. The relevant equations are nonlinear and it is not easy to obtain an exact solution. Generally, iterative arithmetic methods are applied to solve nonlinear equations [1]. A recursive formula for the solution of multilateration systems can be found in [2]. An exact closed-form solution for trilateration systems is presented in [3] where the stations' plane is used as reference and the site of one station is used as the origin of the coordinate frame. Thus, if any other coordinate frame has to be used, transformation has to be applied not only to the position vector estimate but also to the covariance matrix and the mean value of its error vector as well. A closed-form expression has been presented in [4] for the vertical component of the object position vector. However, the formula has not been explicitly derived. Also, no guide lines have been given for the approach followed to obtain this expression. This system has been proposed as one candidate approach for aircraft geometric height monitoring. The concept of the system is to derive the height onboard the aircraft by measuring the distances from three distance measuring equipment (DME) ground stations via the DME interrogation equipment with which the majority of aircraft is equipped. Accurate geometric height monitoring, independent from the barometric altimeter, is required in order to evaluate the height-keeping performance of the current population of aircraft. This is a prerequisite for the reduction of the vertical separation minima for flights performed above 29000 ft [5].

In the next section we derive an explicit, exact and efficient algorithm for estimating the three-dimensional (3-D) position vector based on three range measurements. The key point of the algorithm is that it is performed by two matrix-vector multiplications and a square root operation. The vector elements are simple functions of the ranges only, whereas the matrices are functions of the stations' coordinates. Thus the computation load is kept to a minimum in the case in which the stations are firmly located during the passage of the monitored object, as it holds for the DME-based aircraft height monitoring system. The stations-position related coefficients are calculated only once, at the time the object enters the system data acquisition area, and then are stored for direct use at any subsequent time the new position estimation is to obtained. The algorithm presented in [4] for the vertical component of the position vector is unnecessarily complicated and demands the calculation of many coefficients through cumbersome formulae. Notice that this must be repeatedly performed as the aircraft moves, since the coefficients depend on both the distance measurements and the coordinates of the

stations. The raw position measurements are usually fed to suitable filtering algorithms, such as a Kalman filter, to improve the position accuracy. However, the position measurements are not statistically uncorrelated, so they have to be jointly smoothed [6, 7]. Hence, we propose to derive the complete 3-D position vector, even whether the interest is in one coordinate only, e.g. the vertical component.

Section III copes with the performance of the algorithm. Its simple form facilitates the analysis and explicit expressions for both the variance and the expected value of the position estimation errors are easily derived and provided. Notice that in [3] the subject of performance analysis has not been addressed, whereas in [4] neither analytic expressions have been provided for the variance nor the expected value of position estimation errors has been addressed. As it is proved in this section, the expected value of the position estimation error does not equal zero due to the joint effect of the system nonlinearities and the noise in the distance measurements, although this noise is assumed to have zero mean value. This phenomenon must not be ignored and has to be suitably anticipated for at subsequent measurement data processing phases, such as Kalman filtering. In Section IV we present the performance evaluation results obtained under various typical conditions.

II. EFFICIENT CLOSED-FORM POSITION ESTIMATION ALGORITHM

Let $\mathbf{r}_i = [x_i\ y_i\ z_i]^T$ be the position vector of the ith DME station, $i = 1,2,3$ and, $\mathbf{r}_a = [x\ y\ z]^T$ be the aircraft 3-D position vector. The distance R_i between aircraft and station s_i is expressed in terms of $\mathbf{r}_i$ and $\mathbf{r}_a$ as

$$R_i = ((x-x_i)^2 + (y-y_i)^2 + (z-z_i)^2)^{1/2}. \tag{1}$$

A set of three equations of the above form is available, which is nonlinear in terms of the unknown position vector $\mathbf{r}_a$. The commonly employed method to obtain a solution is the Taylor-series method. With this method the nonlinear set of equations is linearized by expanding it in a Taylor series around a point close enough to the actual position. The linearized system is solved and a new approximation of $\mathbf{r}_a$ is obtained. In the sequel, the new approximate solution is used as the new linearization point and this process is iteratively applied until there is convergence. Drawbacks of the method are that it requires an initial guess close to the actual solution, convergence is not generally assured and, finally, successive iterations imply computation burden.

The alternative approach proposed here is to transform the initial set of equations into another set which can explicitly be solved for the unknown position vector. Specifically, squaring (1) yields

$$R_i^2 = S_i^2 - 2x_i x - 2y_i y - 2z_i z + x^2 + y^2 + z^2 \qquad i = 1,2,3 \tag{2}$$

where

$$S_i^2 = x_i^2 + y_i^2 + z_i^2. \tag{3}$$

Subtracting R_1^2 from R_i^2, $i = 2,3$, we get

$$R_i^2 - R_1^2 = S_2^2 - S_1^2 - 2x_{i1}x - 2y_{i1}y - 2z_{i1}z \qquad i = 2,3 \tag{4}$$

where

$$\begin{aligned} x_{i1} &= x_i - x_1, \\ y_{i1} &= y_i - y_1, \\ z_{i1} &= z_i - z_1. \end{aligned} \tag{5}$$

The set of the two transformed equations can be written in matrix form as

$$\mathbf{W}\mathbf{r}_h = \boldsymbol{\beta} - \mathbf{d}z \tag{6}$$

$$\boldsymbol{\beta} = \begin{bmatrix} \beta_2^2 \\ \beta_3^2 \end{bmatrix} \qquad \mathbf{r}_h = \begin{bmatrix} x \\ y \end{bmatrix}$$

$$\mathbf{d} = \begin{bmatrix} z_{21} \\ z_{31} \end{bmatrix} \qquad \mathbf{W} = \begin{bmatrix} x_{21} & y_{21} \\ x_{31} & y_{31} \end{bmatrix} \tag{7}$$

$$\beta_i^2 = (R_1^2 - R_i^2 - S_1^2 + S_i^2)/2, \qquad i = 2,3.$$

It is readily seen that matrix $\mathbf{W}$ will be singular if and only if the station sites lie on the same line. In the general case, in which the three stations are separately located forming a triangle, the matrix $\mathbf{W}$ will be nonsingular, consequently the aircraft horizontal position $\mathbf{r}_h$ can be expressed as

$$\mathbf{r}_h = \mathbf{W}^{-1}(\boldsymbol{\beta} - \mathbf{d}z). \tag{8}$$

Rewritting (2) at $i = 1$ in the following form

$$R_1^2 = S_1^2 - 2\mathbf{r}_{h1}^T\mathbf{r}_h - 2z_1 z + \mathbf{r}_h^T\mathbf{r}_h + z^2 \qquad \mathbf{r}_{h1} = [x_1 \quad y_1]^T \tag{9}$$

and substituting (8) in (9) we obtain the following quadratic of aircraft vertical position

$$az^2 + bz + c = 0 \tag{10}$$

where

$$a = 1 + \mathbf{d}^T\mathbf{W}^{-T}\mathbf{W}^{-1}\mathbf{d} \tag{11}$$

$$b = 2\mathbf{r}_{h1}^T\mathbf{W}^{-1}\mathbf{d} - 2z_1 - 2\mathbf{d}^T\mathbf{W}^{-T}\mathbf{W}^{-1}\boldsymbol{\beta} \tag{12}$$

$$c = S_1^2 - R_1^2 + \boldsymbol{\beta}^T\mathbf{W}^{-T}\mathbf{W}^{-1}\boldsymbol{\beta} - 2\mathbf{r}_{h1}^T\mathbf{W}^{-1}\boldsymbol{\beta}. \tag{13}$$

Consequently the aircraft height is computed as

$$z = (-b \pm (b^2 - 4ac)^{1/2})/2a. \tag{14}$$

In the sequel, substituting (14) in (8) yields the closed-form expression for horizontal position. Thus, the 3-D position vector can be explicitly calculated from the following expression

$$\mathbf{r}_a = \begin{bmatrix} x \\ y \\ z \end{bmatrix} = \begin{bmatrix} \mathbf{W}^{-1}\boldsymbol{\beta} \\ --- \\ 0 \end{bmatrix} + \begin{bmatrix} -\mathbf{W}^{-1}\mathbf{d} \\ ---- \\ 1 \end{bmatrix} (-b \pm (b^2 - 4ac)^{1/2})/2a. \quad (15)$$

The two altitudes calculated from (14) are mirror symmetric to the plane of the stations, consequently the positive sign is selected in the above solution since the aircraft height z is always positive. Of course if the stations are located on surface ships, one could select the positive or negative sign according to whether the interrogator is in an aircraft or in a submarine.

In [4] the subject of aircraft geometric height estimation based on DME measurements is addressed and a closed-form algorithm is presented which can be found in Appendix A. However, the methodology used to derive the height estimation formula has not been demonstrated. After some algebraic elaboration it can be shown that the quadratic coefficients A, B, C used in Appendix A are equivalent to a, b and c derived in this section. Note that the B and C coefficients, as well as the b and c, have to be evaluated at each time a new set of distance measurements is available, since they depend on both the coordinates of the stations and on the distance measurements. However, the new expressions offer small computational improvements since b and c are now computed using concise matrix-based expressions which are simpler than that of [4]. Notice that $\mathbf{W}$, $\mathbf{d}$, and $\mathbf{r}_{h1}$ depend on the coordinates of the stations only, whereas the array $\boldsymbol{\beta}$ depends on both the distance measurements and the positions of the stations. Consequently, when the reference stations are firmly located, as it holds in the DME case, it is easy to achieve significant computational improvements by a simple further elaboration. For this purpose the vector $\boldsymbol{\beta}$ can be written as

$$\boldsymbol{\beta} = (1/2)(\boldsymbol{\rho} - \boldsymbol{\delta}) \quad (16)$$

where $\boldsymbol{\rho} = [\rho_2^2\ \rho_3^2]^T$, and $\boldsymbol{\delta} = [\delta_2^2\ \delta_3^2]^T$,

$$\rho_i^2 = R_1^2 - R_i^2 \qquad i = 2,3 \quad (17)$$

$$\delta_i^2 = S_1^2 - S_i^2 \qquad i = 2,3. \quad (18)$$

Substituting (16) in (15), and after some algebraic operations shown in Appendix B, the 3-D position estimate can be obtained by the following simple expression

$$\mathbf{r}_a = \mathbf{f}(\mathbf{r}) = \boldsymbol{\Lambda}\mathbf{u} + \boldsymbol{\mu}(\boldsymbol{\xi}^T\mathbf{v})^{1/2}$$

$$\boldsymbol{\Lambda} = \begin{bmatrix} \boldsymbol{\lambda}_1^T \\ \boldsymbol{\lambda}_2^T \\ \boldsymbol{\lambda}_3^T \end{bmatrix}$$

$$\boldsymbol{\lambda}_i^T = [\lambda_{i0}\ \ \lambda_{i1}\ \ \lambda_{i1}\ \ \lambda_{i1}]$$

$$\boldsymbol{\mu} = \begin{bmatrix} \mu_1 \\ \mu_2 \\ \mu_3 \end{bmatrix} \quad (19)$$

$$\boldsymbol{\xi} = [\xi_0\ \ \xi_1\ \ \cdots\ \ \xi_9]^T$$

$$\mathbf{u} = [1\ \ R_1^2\ \ R_2^2\ \ R_3^2]^T$$

$$\mathbf{v} = [1\ \ R_1^2\ \ R_2^2\ \ R_3^2\ \ R_1^4\ \ R_2^4\ \ R_3^4\ \ R_1^2R_2^2\ \ R_1^2R_3^2\ \ R_2^2R_3^2]^T$$

where $\mathbf{r}$ denotes the range measurement array, $\mathbf{r} = [R_1\ R_2\ R_3]^T$. Notice that the distance measurements involve only in vectors $\mathbf{u}$ and $\mathbf{v}$. The expressions for the elements $\lambda_{ij}, \mu_i, \xi_i$ of $\boldsymbol{\Lambda}$, $\boldsymbol{\mu}$, and $\boldsymbol{\xi}$ can be found in Appendix B. These elements are completely determined by the station location coordinates, consequently, since the latter are firmly located, they are calculated only once at the moment the aircraft enters the data acquisition area. In the sequel, they can be directly used at any subsequent time the 3-D position estimate is required.

The comparison of the new 3-D estimation algorithm expressed by (19) with the height estimation algorithm proposed in [4], shows that the new algorithm is drastically improved. First, it gives a solution to the 3-D position estimation problem. However, the major benefit is that the computation burden has significantly been reduced, since few simple arithmetic operations suffice to estimate the position due to the appropriate formulation and effective use of constant stations-position-dependent coefficients. In contrast, the height computation algorithm of [4] necessitates a lot of cumbersome calculations which must repeatedly be performed each time a new set of range measurements is received, since it is based on many coefficients which are varying with aircraft movement. The same remarks hold when the new algorithm compares with the 3-D estimation algorithm proposed in [3], even though the expressions proposed are simpler than that of [4]. Notice that the solution derived in [3] is expressed according to a specific coordinate frame. Namely, the XY plane is the plane of the stations, the X axis is defined by one baseline and the origin of the frame is at the end of the X axis baseline. Thus, if any other coordinate system has to be used, additional operations are required

for the position vector transformation as well as for the transformation of the covariance matrix and the expected value of the corresponding error vector.

Another interesting aspect of the new algorithm is that it is mathematically more tractable. Thus, it accommodates a more thorough investigation of the effects caused on calculated height by both the geometry and the random ranging errors.

III. PERFORMANCE ANALYSIS

Let δR_i, R_{i0} denote the additive random error and the actual value of distance measurement R_i, respectively. Let $\delta \mathbf{r} = [\delta R_1 \ \delta R_2 \ \delta R_3]^T$ and $\mathbf{r_0} = [R_{10} \ R_{20} \ R_{30}]^T$ be brief array notations for the sets of measurement errors and the actual values of distances. The following relation holds

$$\mathbf{r} = \mathbf{r_0} + \delta \mathbf{r}. \tag{20}$$

Let $\mathbf{S}$ denote the covariance matrix of the random error vector $\delta \mathbf{r}$. The errors are assumed to have zero mean value, that is

$$E\{\delta \mathbf{r}\} = \mathbf{0}$$

where $E\{\cdot\}$ stands for the expected value operation. Obviously the use of noisy input data in the position estimating expression (19) results in an error $\delta \mathbf{r}_a$ known as equation error defined as

$$\delta \mathbf{r}_a = \mathbf{r}_a - \mathbf{r}_{a0} \tag{21}$$

where $\mathbf{r}_{a0} = \mathbf{f}(\mathbf{r_0})$ is the actual aircraft position and $\delta \mathbf{r}_a = [\delta x \ \delta y \ \delta z]^T$.

The function relating the position estimate to the noisy measurements is nonlinear, consequently $E\{\delta \mathbf{r}_a\} \neq 0$, thus the estimates derived will be biased. The bias is inherently generated by the nonlinear processing of noisy measurements; even the noise has zero mean value [8]. The existence of biased position estimates have been shown by computer simulations in [9, 10] and analytically in [11–15]. To evaluate the bias, we expand each element of the explicit-solution expression into a Taylor series around $\mathbf{r_0}$. Thus, for the x coordinate, the $f_1(\mathbf{r})$ is expanded as

$$x = f_1(\mathbf{r}) = f_1(\mathbf{r_0}) + \sum_{i=1}^{3} \frac{\partial f_1}{\partial R_i} \delta R_i + \frac{1}{2} \sum_{i=1}^{3} \sum_{j=1}^{3} \frac{\partial^2 f_1}{\partial R_i \partial R_j} \delta R_i \delta R_j + \varepsilon_1 \tag{22}$$

where the partial derivatives are evaluated at the mean value $\mathbf{r_0}$. For small measurement errors the higher order terms ε_1 can be neglected and the function can be well approximated by retaining the terms up to the second-order partial derivatives. Taking the expected values of (22) and using (21) the expected value of random error in x coordinate, i.e., the bias b_x, is

$$b_x = E\{\delta x\} = E\{x\} - x_0 = \frac{1}{2} \sum_{i=1}^{3} \sum_{j=1}^{3} \frac{\partial^2 f_1}{\partial R_i \partial R_j} s_{ij} = \tfrac{1}{2} \mathrm{tr}(\mathbf{D_1 S}) \tag{23}$$

where s_{ij} is element of the covariance matrix $\mathbf{S}$, and $\mathrm{tr}(\cdot)$ stands for the trace operator. The second-order partial derivatives matrix $\mathbf{D}_1$ is easy to evaluate due to the simple form of function $f_1(\mathbf{r})$, specifically:

$$\begin{aligned} \mathbf{D}_1 &= \frac{\partial^2 f_1}{\partial \mathbf{r}^2} = \frac{\partial^2 (\boldsymbol{\lambda}_1^T \mathbf{u})}{\partial \mathbf{r}^2} + \mu_1 \frac{\partial^2 (\boldsymbol{\xi}^T \mathbf{v})^{1/2}}{\partial \mathbf{r}^2} \\ &= 2\mathbf{L}_1 + \mu_1 \frac{1}{4(\boldsymbol{\xi}^T \mathbf{v})^{1/2}} (2\boldsymbol{\xi}^T \mathbf{v} \boldsymbol{\psi} - \mathbf{g}\mathbf{g}^T) \\ \mathbf{L}_1 &= \mathrm{diag}(\lambda_{11} \quad \lambda_{12} \quad \lambda_{13}) \\ \mathbf{g} &= \frac{\partial (\boldsymbol{\xi}^T \mathbf{v})}{\partial \mathbf{r}} \qquad \boldsymbol{\psi} = \frac{\partial^2 (\boldsymbol{\xi}^T \mathbf{v})}{\partial \mathbf{r}^2}. \end{aligned} \tag{24}$$

Similarly the expression for the bias in the y coordinate is $b_y = (1/2)\mathrm{tr}(\mathbf{D_2 S})$ where $\mathbf{D}_2$ is obtained by substituting $\mathbf{L}_2 = \mathrm{diag}(\lambda_{21} \ \lambda_{22} \ \lambda_{23})$ for $\mathbf{L}_1$ and μ_2 for μ_1 in (24). The systematic error in the z coordinate is similarly evaluated. The specific elements of g and ψ are not shown since it is easy to derive them due to the simple polynomial-type form of $\boldsymbol{\xi}^T \mathbf{v}$.

The covariance matrix $\mathbf{P}$ of the position estimate error $\delta \mathbf{r}_a$ can now be evaluated as

$$\begin{aligned} \mathbf{P} &= E\{[\delta \mathbf{r}_a - E\{\delta \mathbf{r}_a\}][\delta \mathbf{r}_a - E\{\delta \mathbf{r}_a\}]^T\} \\ &= E\{\delta \mathbf{r}_a \delta \mathbf{r}_a^T\} - E\{\delta \mathbf{r}_a\} E\{\delta \mathbf{r}_a^T\} \\ &= \mathbf{F S F}^T - E\{\delta \mathbf{r}_a\} E\{\delta \mathbf{r}_a^T\} \\ \mathbf{F} &= \frac{\partial \mathbf{f}}{\partial \mathbf{r}} = \frac{\partial (\boldsymbol{\Lambda} \mathbf{u})}{\partial \mathbf{r}} + \mu \frac{\partial (\boldsymbol{\xi}^T \mathbf{v})^{1/2}}{\partial \mathbf{r}} \\ &= 2\mathbf{L}\mathbf{R}_d + \frac{1}{2(\boldsymbol{\xi}^T \mathbf{v})^{1/2}} \mu \mathbf{g}^T \end{aligned} \tag{25}$$

where $\mathbf{L}$ is a 3×3 matrix defined by the last three columns of $\boldsymbol{\Lambda}$, i.e., $l_{ij} = \lambda_{ij}$ $(i, j = 1,2,3)$, and $\mathbf{R}_d = \mathrm{diag}(R_1 \ R_2 \ R_3)$. The diagonal elements of $\mathbf{P}$ contain the variances σ_x^2, σ_y^2, and σ_z^2 of the estimation errors along each axis, whereas the off-diagonal elements represent their cross-correlation.

The performance of the algorithm is affected by the ranging errors and by the geometrical arrangement of the stations and aircraft relative position. The geometry causes the Dilution Of Precision (DOP) effect, i.e., the ranging error amplification when the position vector is computed. Assume that the range measurement errors are uncorrelated with the same variance σ^2. Consequently their covariance matrix can be expressed as $\mathbf{S} = \mathbf{I}\sigma^2$, where $\mathbf{I}$ denotes the identity matrix. Under the above assumptions the following

performance indices can be defined

$$\text{GDOP} = \frac{\sqrt{\sigma_x^2 + \sigma_y^2 + \sigma_z^2}}{\sigma} = \frac{\sqrt{\text{tr}(\mathbf{P})}}{\sigma}$$

$$\text{HDOP} = \frac{\sqrt{\sigma_x^2 + \sigma_y^2}}{\sigma}$$

where geometric DOP (GDOP) is a general performance index, horizontal DOP (HDOP) is the performance index for the XY plane position estimation. In a similar manner, the standard deviation (SD) of the vertical position estimation error can be evaluated as

$$\sigma_z = (\text{VDOP}) \cdot \sigma \tag{26}$$

where VDOP is the vertical DOP. The above performance indices express the effect of the geometry and can be considered as normalized SD errors. Similarly applying the above assumptions to the bias evaluation formula (23), it yields that the position estimation systematic errors for each coordinate can be expressed as

$$b_x = B_x\sigma^2 \qquad b_y = B_y\sigma^2 \qquad b_z = B_z\sigma^2 \tag{27}$$

where B_x, B_y, and B_z are geometric factors expressing the effect of the system nonlinearities and can be referred to as normalized biases. Another performance index is the total bias b_t and the normalized total bias B_t, defined as

$$b_t = B_t\sigma^2 \qquad B_t = \sqrt{b_x^2 + b_y^2 + b_z^2}. \tag{28}$$

Notice that the SD of the position estimation error is proportional to the SD of the ranging errors, whereas the estimation biases are proportional to the square of the ranging errors.

IV. PERFORMANCE EVALUATION

The general effect of various parameters can be examined by the representative case in which the XY coordinates of the sites of the stations form an equilateral triangle inscribed in a circle with radius l. The latter can be referred to as the system baseline. The origin of the coordinate frame is at the center of the triangle. Thus the location vectors of the stations are $\mathbf{r}_{h1} = [-l\sqrt{3}/2, -l/2]^T$, $\mathbf{r}_{h2} = [0, l]^T$, and $\mathbf{r}_{h3} = [l\sqrt{3}/2, -l/2]^T$. The data acquisition area of the system is an XY plane square area, at a height of 8 km, spanning in each direction from −40 km to 40 km.

Figs. 1 and 2 have been derived assuming l = 10 km and $z_1 = 0$ m, $z_2 = -30$ m, and $z_3 = 50$ m. Fig. 1 shows constant-DOP isograms for 3-D, horizontal, and vertical position estimation errors. It is seen that the HDOP depends on the distance only from the center of the stations. The VDOP is affected by both the distance and the relative position on the

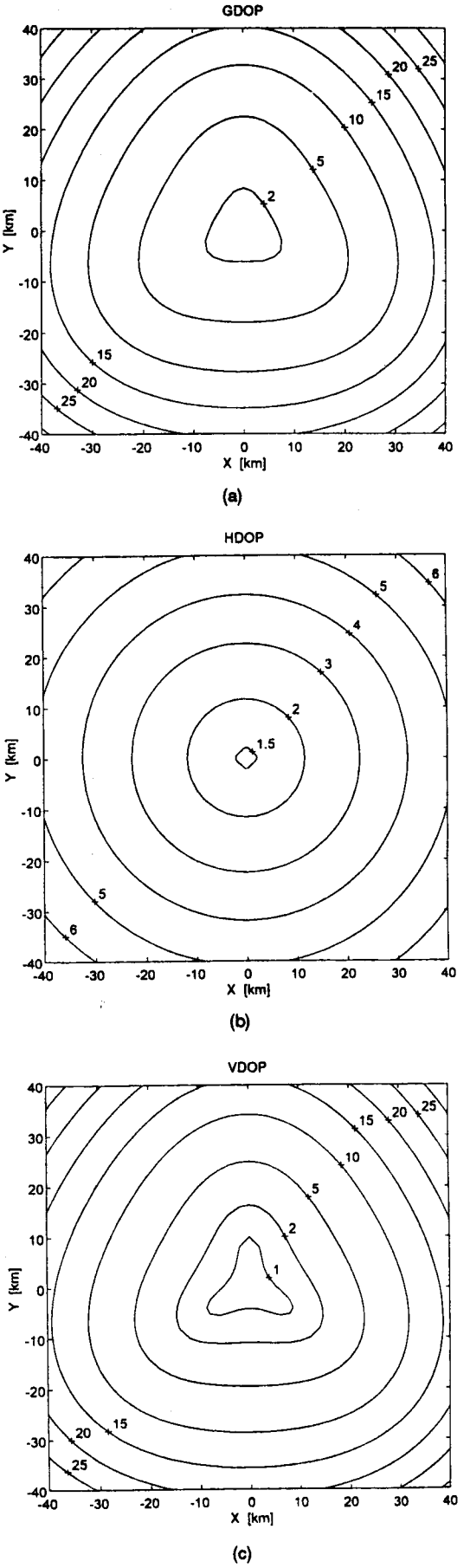

Fig. 1. Constant-DOP isograms (l = 10 km).

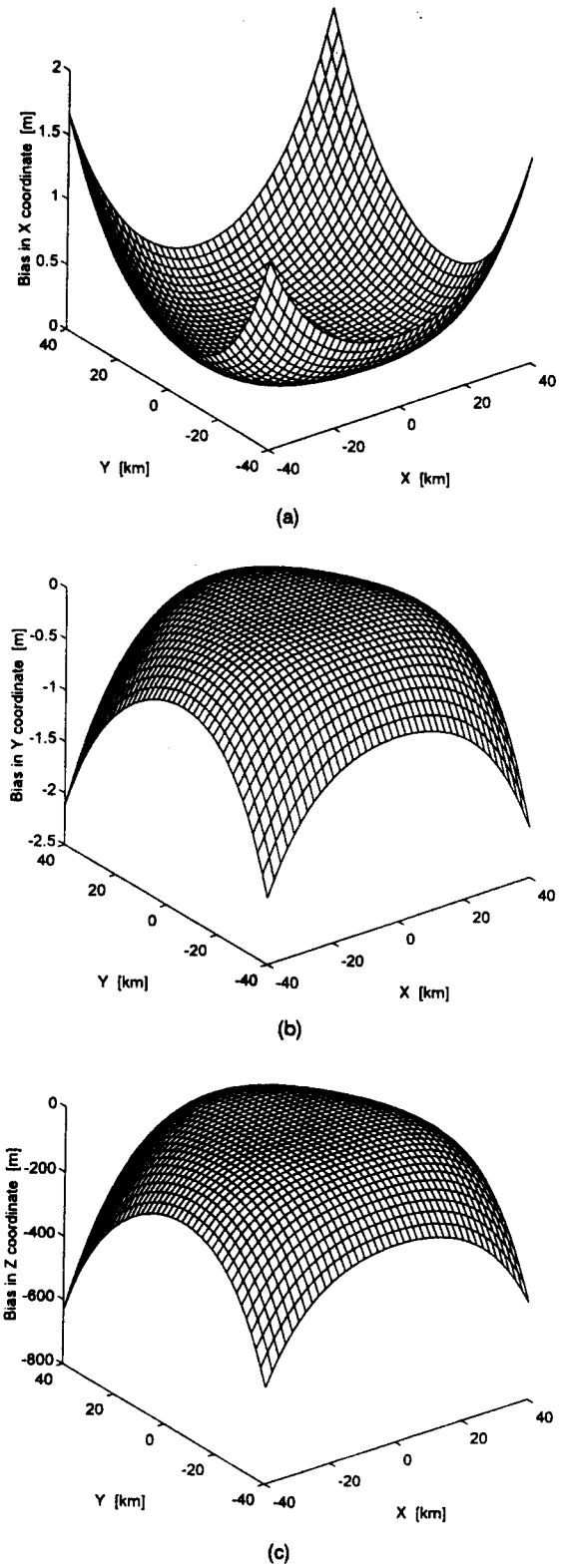

Fig. 2. Systematic errors in position estimates ($l = 10$ km, $\sigma = 90$ m).

XY mesh. However, the relative position has reduced influence for larger distances since, as it can be seen in Fig. 1(c), the shape of the curves tends to be more circular as the distance increases. From the comparison of Figs. 1(b) and 1(c) it is seen that, for distances close to the center, the HDOP and VDOP actually present the same values. However, as the distance from the center increases, the VDOP increases more rapidly and presents significantly larger values than the HDOP. Also, the comparison with Fig. 1(a) corroborates that, for large distances, the vertical component of the error vector becomes the dominant contributor to the GDOP. It is important to notice that Fig. 1(c) shows that there is a small area in which VDOP equals one, which means that σ_z is exclusively determined by the ranging errors SD, which for normal DME equals 90 m, whereas for PDME (precision DME) it is $\sigma = 20$ m.

Fig. 2 shows the corresponding systematic estimation errors for each direction when normal DMEs are used. It is seen that the biases in the horizontal position estimates are negligible and can be ignored almost for all the extent of the data acquisition area. However, the bias in vertical position estimates cannot be ignored since it retains large values even close to the center of the stations' arrangement. It is seen in Fig. 2(c) that, although the aircraft is assumed flying at constant altitude, the height measurements produced by the position estimation algorithm will erroneously indicate that it ascends and descends when it approaches to, and goes away from, the stations' formation center, respectively. This effect must be taken into account in the subsequent algorithms utilizing these measurements for comparison with pressure altimeter measurements or for obtaining more accurate smoothed height estimates. For example, if a Kalman filter is to be employed, the filter designer has to incorporate the systematic errors in the appropriate system modeling. Notice that the usual Kalman filter proposed in [4] does not correctly model the measurement process and consequently yields biased height estimates. From Figs. 1 and 2 it is concluded that the geometry affects the system performance more strongly in the vertical direction than in the horizontal plane.

Figs. 3 and 4 show the effect of the system baseline length. The constant-GDOP isograms seen in Fig. 3 show that the baseline is an important factor. The larger the baseline is, so much the better the system performance is, especially for increased distances from the center. Marginal improvement is observed for areas close to stations arrangement. However, the comparison of Fig. 3(c) with Fig. 3(b) and Fig. 1(a) shows that there is a critical length when increasing the baseline. Increasing the baseline beyond the critical length results in a small performance deterioration for areas close to center, although improved performance is achieved for wider areas. Specifically, Fig. 3(c) shows that, when $l = 30$ km, GDOP equals 3 for the most part of the central area and GDOP equals 2 for small areas restricted in the neighborhood of the stations, whereas Fig. 3(b) shows that, when $l = 20$ km, GDOP equals 2 for larger area than that of Fig. 3(c).

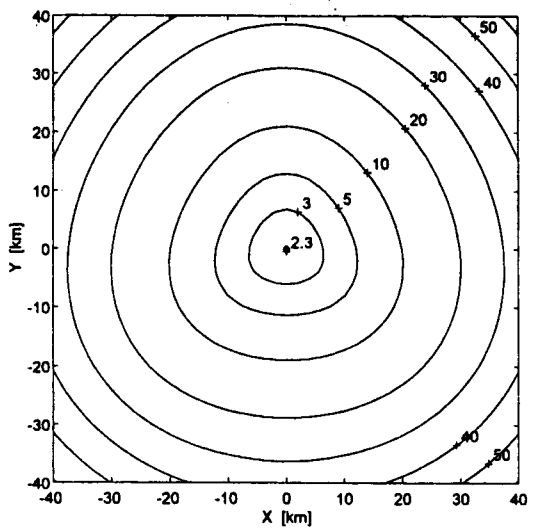

(a)

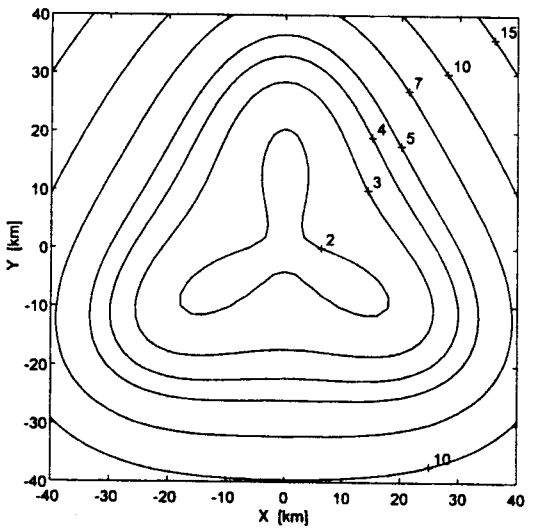

(b)

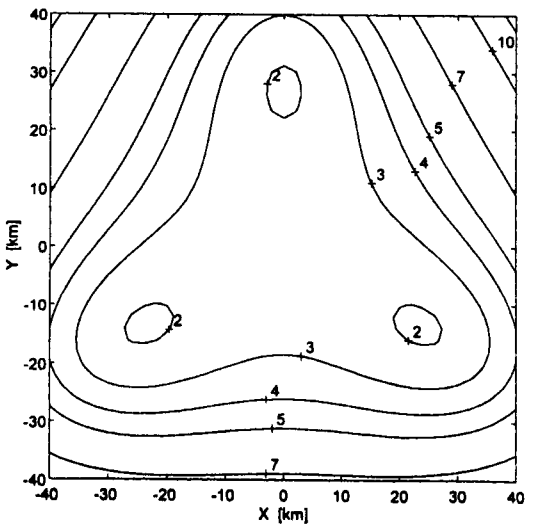

(c)

Fig. 3. Constant-GDOP isograms for various baseline lengths. (a) $l = 5$ km. (b) $l = 20$ km. (c) $l = 30$ km.

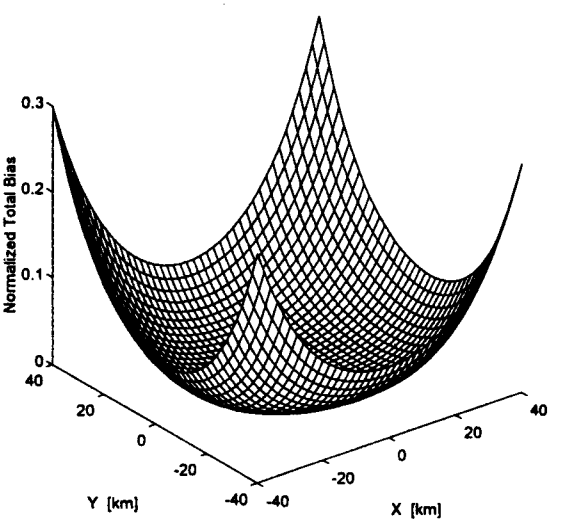

(a)

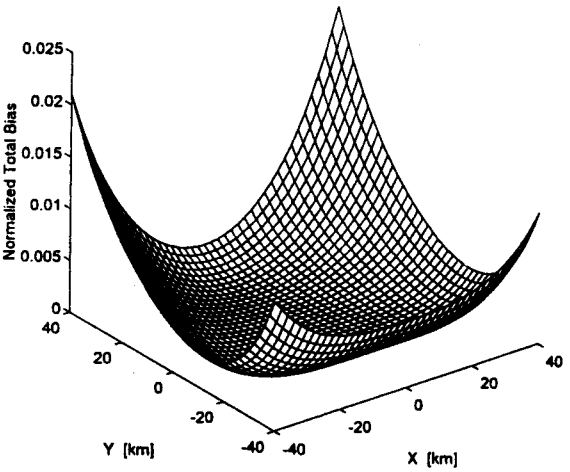

(b)

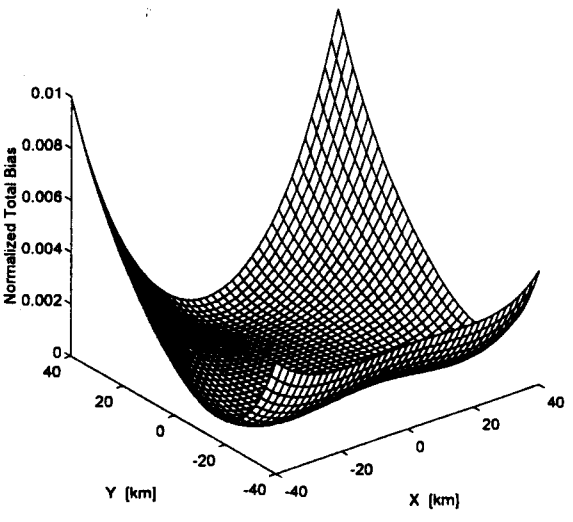

(c)

Fig. 4. Normalized total systematic errors in position estimates for various baseline lengths. (a) $l = 5$ km. (b) $l = 20$ km. (c) $l = 30$ km.

Thus, if the data acquisition length is restricted to 30 km (from −15 km to 15 km), a baseline of 20 km is preferable rather than that of 30 km. However, the second baseline must be used if the data collection is conducted for larger paths or at higher flight levels. Fig. 4 shows the normalized total bias B_t. Observe that, as it results from (28) and plots of Fig. 2, the main contributor to B_t is the bias in the vertical direction. Notice also, that the bias is obtained by multiplying the normalized bias by σ^2. Hence, for a baseline of 5 km and for the data acquisition area considered herein, the total bias reaches values up to 2340 m for normal DMEs and up to 120 m for PDMEs.

V. CONCLUSIONS

We presented a new explicit solution to the problem for 3-D position estimation based on three range measurements. The algorithm is computationally efficient since it requires a few simple arithmetic operations. The second advantage offered is that it facilitates a more thorough mathematical performance analysis. Analytical expressions have easily been derived for both the variance and expected value of measurement errors. The performance evaluation has been conducted for a 3-D position monitoring system operating onboard an aircraft and based on three DME ground stations. The evaluation has shown that the system geometry affects more strongly the performance in the vertical direction than that in the horizontal plane. The biases in horizontal plane position estimates can be ignored. In the vertical direction however, large values hold for the systematic error, even with the use of precision DMEs, thus it cannot be ignored if highly accurate vertical position estimates are required.

APPENDIX A. PREVIOUS HEIGHT COMPUTATION ALGORITHM

In [4] the following closed-form algorithm was presented for computing the aircraft height z based on three range measurements R_1, R_2, and R_3:

$$z = \frac{-B + (B^2 - 4AC)^{1/2}}{2A}$$

$$A = \frac{4A_1^2 - A_2^2 A_3}{A_4}$$

$$B = \frac{4A_1 B_1 - A_2^2 B_2}{A_4}$$

$$C = \frac{B_1^2 - A_2^2 C_1}{A_4}.$$

To evaluate the terms A_i, B_i, and C_1, first define the following quantities

$$x_{21} = x_2 - x_1$$

$$y_{21} = y_2 - y_1$$

$$z_{21} = z_2 - z_1$$

$$K_1 = R_1^2 - (x_1^2 + y_1^2 + z_1^2)$$

$$K_2 = R_2^2 - (x_2^2 + y_2^2 + z_2^2)$$

$$K_3 = R_3^2 - (x_3^2 + y_3^2 + z_3^2)$$

and then compute them according to

$$\begin{aligned} A_1 = {} & -x_1 x_{21} y_{21}^2 z_{21} - x_1 x_{21}^3 z_{21} - y_1 x_{21}^2 y_{21} z_{21} - y_1 y_{21}^3 z_{21} \\ & + z_1 y_{21}^4 + z_1 x_{21}^4 + x_3 x_{21}^3 z_{21} + x_3 x_{21} y_{21}^2 z_{21} \\ & + y_3 x_{21}^2 y_{21} z_{21} - z_3 x_{21}^4 - 2 z_3 x_{21}^2 y_{21}^2 - z_3 y_{21}^4 \\ & + y_3 y_{21}^3 z_{21} + 2 z_1 x_{21}^2 y_{21}^2 \end{aligned}$$

$$\begin{aligned} A_2 = {} & x_1 y_{21}^3 - y_1 x_{21} y_{21}^2 - x_3 x_{21}^2 y_{21} - x_3 y_{21}^3 \\ & + x_1 x_{21}^2 y_{21} - y_1 x_{21}^3 + y_3 x_{21} y_{21}^2 + y_3 x_{21}^3 \end{aligned}$$

$$A_3 = -4(x_{21}^2 + y_{21}^2 + z_{21}^2)$$

$$A_4 = (x_{21}^2 + y_{21}^2)^4$$

$$\begin{aligned} B_1 = {} & 2x_1^2 y_{21}^4 + 2y_1^2 x_{21}^2 y_{21}^2 + x_1(K_1 - K_2) x_{21} y_{21}^2 - K_3 y_{21}^4 \\ & + y_1(K_1 - K_2) x_{21}^2 y_{21} - 4 x_1 y_1 x_{21} y_{21}^3 \\ & + y_1(K_1 - K_2) y_{21}^3 - x_3(K_1 - K_2) x_{21}^3 - 2 x_1 x_3 x_{21}^2 y_{21}^2 \\ & - x_3(K_1 - K_2) x_{21} y_{21}^2 + 2 x_3 y_1 x_{21}^3 y_{21} - 2 x_1 x_3 y_{21}^4 \\ & - 2 y_1 y_3 x_{21}^2 y_{21}^2 - K_3 x_{21}^4 + 2 x_3 y_1 x_{21} y_{21}^3 \\ & + 2 x_1^2 x_{21}^2 y_{21}^2 + 2 y_1^2 x_{21}^4 - 4 x_1 y_1 x_{21}^3 y_{21} \\ & + K_1 x_{21}^4 + x_1(K_1 - K_2) x_{21}^3 - y_3(K_1 - K_2) x_{21}^2 y_{21} \\ & + 2 x_1 y_3 x_{21} y_{21}^3 + 2 x_1 y_3 x_{21}^3 y_{21} - 2 y_1 y_3 x_{21}^4 \\ & - y_3(K_1 - K_2) y_{21}^3 + 2 K_1 x_{21}^2 y_{21}^2 \\ & + K_1 y_{21}^4 - 2 K_3 x_{21}^2 y_{21}^2 \end{aligned}$$

$$\begin{aligned} B_2 = {} & 4(-2 y_1 y_{21} z_{21} + 2 z_1 x_{21}^2 + (K_1 - K_2) z_{21} \\ & - 2 x_1 x_{21} z_{21} + 2 z_1 y_{21}^2) \end{aligned}$$

$$\begin{aligned} C_1 = {} & 4x_1^2 y_{21}^2 + 4y_1^2 x_{21}^2 + 4y_1(K_1 - K_2) y_{21} - 8 x_1 y_1 x_{21} y_{21} \\ & + 4 K_1 x_{21}^2 + 4 K_1 y_{21}^2 - (K_1 - K_2)^2 \\ & + 4(K_1 - K_2) x_1 x_{21}. \end{aligned}$$

APPENDIX B. EFFECTIVE FORMULATION OF 3-D POSITION ESTIMATION ALGORITHM

Using (16)–(18) in (14) and after some elaboration yields

$$z = \boldsymbol{\lambda}^T \mathbf{u} \pm (\boldsymbol{\xi}^T \mathbf{v})^{1/2} \tag{29}$$

where

$$\mathbf{u} = [1 \quad R_1^2 \quad R_2^2 \quad R_3^2]^T$$

$$\mathbf{v} = [1 \quad R_1^2 \quad R_2^2 \quad R_3^2 \quad R_1^4 \quad R_2^4 \quad R_3^4 \quad R_1^2R_2^2 \quad R_1^2R_3^2 \quad R_2^2R_3^2]^T$$

$$\boldsymbol{\lambda}^T = [\lambda_0 \quad \lambda_1 \quad \lambda_2 \quad \lambda_3]$$

$$\boldsymbol{\xi}^T = [\xi_0 \quad \xi_1 \quad \cdots \quad \xi_9].$$

The elements of $\boldsymbol{\lambda}$ and $\boldsymbol{\xi}$ are determined by the DME position coordinates. Specifically, define matrix $\mathbf{G}$ and array $\mathbf{e}$ as

$$\mathbf{G} = \mathbf{W}^{-T}\mathbf{W}^{-1}$$

$$\mathbf{e}^T = (1/2)\delta^T\mathbf{W}^{-T}\mathbf{W}^{-1} + \mathbf{r}_{h1}^T\mathbf{W}^{-1}$$

and then compute λ_i and ξ_i using the following expressions

$$\lambda_0 = -(2\mathbf{r}_{h1}^T\mathbf{W}^{-1}\mathbf{d} - 2z_1 + \mathbf{d}^T\mathbf{W}^{-T}\mathbf{W}^{-1}\delta)/2a$$

$$\lambda_1 = (z_{21}(g_{11} + g_{12}) + z_{31}(g_{22} + g_{12}))/2a$$

$$\lambda_2 = -(z_{21}g_{11} + z_{31}g_{12})/2a$$

$$\lambda_3 = -(z_{31}g_{22} + z_{21}g_{12})/2a$$

$$\xi_0 = \lambda_0^2 - (\delta^T\mathbf{W}^{-T}\mathbf{W}^{-1}\delta/4 + \mathbf{r}_{h1}^T\mathbf{W}^{-1}\delta + S_1^2)/a$$

$$\xi_1 = 2\lambda_0\lambda_1 + (1 + e_1 + e_2)/a$$

$$\xi_2 = 2\lambda_0\lambda_2 - e_1/a$$

$$\xi_3 = 2\lambda_0\lambda_3 - e_2/a$$

$$\xi_4 = \lambda_1^2 - (g_{11} + 2g_{12} + g_{22})/4a$$

$$\xi_5 = \lambda_2^2 - g_{11}/4a$$

$$\xi_6 = \lambda_3^2 - g_{22}/4a$$

$$\xi_7 = 2\lambda_1\lambda_2 + (g_{11} + g_{12})/2a$$

$$\xi_8 = 2\lambda_1\lambda_3 + (g_{22} + g_{12})/2a$$

$$\xi_9 = 2\lambda_2\lambda_3 - g_{12}/2a.$$

Substituting (29) for the quadratic solution in (15) and using (16)–(18), the 3-D position closed-form solution becomes

$$\mathbf{r}_a = \boldsymbol{\Lambda}\mathbf{u} + \mu(\boldsymbol{\xi}^T\mathbf{v})^{1/2}. \tag{30}$$

Let $\boldsymbol{\lambda}_i^T$ denote the ith row of $\boldsymbol{\Lambda}$ and let $\mathbf{w}_1^T$ and $\mathbf{w}_2^T$ stand for the first and second row of $\mathbf{W}^{-1}$. Then the expressions for $\boldsymbol{\lambda}_i^T$ and μ are

$$\boldsymbol{\lambda}_1 = \begin{bmatrix} -\mathbf{w}_1^T\mathbf{d}\boldsymbol{\lambda} + \dfrac{-\mathbf{w}_1^T\delta}{2} \\ -\mathbf{w}_1^T\mathbf{d}\boldsymbol{\lambda} + \dfrac{y_{31} - y_{21}}{2\det(\mathbf{W})} \\ -\mathbf{w}_1^T\mathbf{d}\boldsymbol{\lambda} + \dfrac{-y_{31}}{2\det(\mathbf{W})} \\ -\mathbf{w}_1^T\mathbf{d}\boldsymbol{\lambda} + \dfrac{y_{21}}{2\det(\mathbf{W})} \end{bmatrix}$$

$$\boldsymbol{\lambda}_2 = \begin{bmatrix} -\mathbf{w}_2^T\mathbf{d}\boldsymbol{\lambda} + \dfrac{-\mathbf{w}_2^T\delta}{2} \\ -\mathbf{w}_2^T\mathbf{d}\boldsymbol{\lambda} + \dfrac{x_{21} - x_{31}}{2\det(\mathbf{W})} \\ -\mathbf{w}_2^T\mathbf{d}\boldsymbol{\lambda} + \dfrac{-x_{31}}{2\det(\mathbf{W})} \\ -\mathbf{w}_2^T\mathbf{d}\boldsymbol{\lambda} + \dfrac{-x_{21}}{2\det(\mathbf{W})} \end{bmatrix}$$

$$\boldsymbol{\lambda}_3 = \boldsymbol{\lambda}$$

$$\mu = [\pm(-\mathbf{w}_1^T\mathbf{d}) \quad \pm(-\mathbf{w}_2^T\mathbf{d}) \quad \pm 1]^T.$$

REFERENCES

[1] Foy, W. H. (1976)
Position-location solutions by Taylor-series estimation.
IEEE Transactions on Aerospace and Electronic Systems, **AES-12**, 2 (Mar. 1976), 187–194.

[2] Grokinski, H. L. (1959)
Position estimation using only multiple simultaneous range measurements.
IRE Transactions on Aeronautical and Navigational Electronics, **ANE-6** (Sept. 1959), 178–187.

[3] Fang, B. T. (1986)
Trilateration and extension to Global Positioning System Navigation.
Journal of Guidance, Control and Dynamics, **9**, 6 (Nov.–Dec. 1986), 715–717.

[4] Rekkas, C. M., Lefas, C. C., and Krikelis, N. J. (1990)
Improving the accuracy of aircraft absolute altitude estimation using DME measurements.
International Journal of Systems Science, **21**, 7 (Jul. 1990), 1381–1392.

[5] Cox, M. E., Ten Have, J. M., and Forrester, D. A. (1991)
European studies to investigate the feasibility of using 1000 ft vertical separation minima.
Journal of Navigation, **44**, 2 (1991), 171–183.

[6] Gelb, A. (1974)
Applied Optimal Estimation.
Cambridge, MA: MIT Press, 1988, tenth printing.

[7] Spingarn, K., and Weidemann, H. L. (1972)
Linear regression filtering and prediction for tracking maneuvering aircraft targets.
IEEE Transactions on Aerospace and Electronic Systems, **AES-8** (Nov. 1972), 800–810.

[8] Papoulis, A. (1984)
Probability, Random Variables and Stochastic Processes (2nd ed.).
New York: McGraw-Hill, 1984.

[9] Manolakis, D. E., and Lefas, C. C. (1994)
Aircraft geometric height computation using secondary surveillance range differences.
IEE Proceedings—Radar, Sonar and Navigation, **141**, 2 (Apr. 1994), 119–124.

[10] Nagaoka, S. (1990)
Possibility of detecting a non-level-flight aircraft by the Navigation Accuracy Measurement System (NAMS).
ICAO RGCSP, Review of the General Concept of Separation Panel, seventh meeting, Montreal, 30/10/90, WP/180.

[11] Gavish, M., and Weiss, A. J. (1992)
Performance analysis of bearing-only target location algorithms.
IEEE Transactions on Aerospace and Electronic Systems, **28**, 3 (July 1992), 817–828.

[12] Manolakis, D. E., Lefas, C. C., Stavrakakis, G. S., and Rekkas, C. M. (1992)
Computation of aircraft geometric height under radar surveillance.
IEEE Transactions on Aerospace and Electronic Systems, **28**, 1 (Jan. 1992), 241–248.

[13] Manolakis, D. E., and Lefas, C. C. (1993)
Systematic errors in ground referenced geometric height monitoring.
IEE Proceedings, Pt. F (Radar and Signal Processing), **140**, 2 (April 1993), 138–144.

[14] Manolakis, D. E., Lefas, C. C., and Dounis, A. I. (1994)
Inherent bias assessment in height computation employing mixed-type radar data.
IEEE Transactions on Aerospace and Electronic Systems, **30**, 4 (Oct. 1994), 1045–1049.

[15] Ho, K. C., and Chan, Y. T. (1993)
Solution and performance analysis of geolocation by TDOA.
IEEE Transactions on Aerospace and Electronic Systems, **29**, 4 (Oct. 1993), 1311–1322.

Dimitris E. Manolakis (M'91) was born in Salonica, Greece, in 1960. He received his Diploma in electrical engineering from the University of Patras, Greece, in 1983 and his Ph.D. in electronics and computer engineering from the Technical University of Crete, Chania, Greece.

From 1986 and 1990 he was a research assistant at the Institute of Informatics and Telecommunications of the "Democritos" National Research Center, Athens. He has worked as Assistant Professor with the Department of Computer Systems in the Technical Educational Institute of Pireaus, Greece, From 1993 to 1994 he worked part-time as a professor with the Department of Electronics Engineering of the Greek Airforce Academy, Athens and as a consultant with Sithon Research Ltd., Athens, Greece. Dr. Manolakis is currently an Associate Professor with the Department of Automation at the Technical Educational Institute of Salonica, Greece. He has performed work in tracking algorithms, position estimation, and the use of the SSR mode S and satellite link for ATC. His general research interests lie in the areas of estimation theory, DSP, sensor data fusion, and fuzzy logic applications.

Dr. Manolakis is a member of the Technical Chamber of Greece (TEE).